Symmetric inseparability and number entanglement in charge-conserving mixed states

Zhanyu Ma,[1] Cheolhee Han,[1] Yigal Meir,[2,3] and Eran Sela[1]
[1]*School of Physics and Astronomy, Tel Aviv University, Tel Aviv 6997801, Israel*
[2]*Department of Physics, Ben-Gurion University of the Negev, Beer Sheva 84105, Israel*
[3]*The Ilse Katz Institute for Nanoscale Science and Technology, Ben-Gurion University of the Negev, Beer Sheva 84105, Israel*

(Received 31 October 2021; revised 8 February 2022; accepted 9 March 2022; published 11 April 2022)

We explore sufficient conditions for inseparability in mixed states with a globally conserved charge, such as a particle number. We argue that even separable states may contain entanglement in fixed charge sectors, as long as the state cannot be separated into charge-conserving components. As a witness of symmetric inseparability we study the number entanglement (NE), ΔS_m, defined as the entropy change due to a subsystem's charge measurement. Whenever $\Delta S_m > 0$, there exist inseparable charge sectors, having finite (logarithmic) negativity, even when the full state either is separable or has vanishing negativity. We demonstrate that the NE is not only a witness of symmetric inseparability, but also an entanglement monotone. Finally, we study the scaling of ΔS_m in thermal one-dimensional systems combining high-temperature expansion and conformal field theory.

DOI: 10.1103/PhysRevA.105.042416

I. INTRODUCTION

Quantifying and exploiting quantum entanglement is a central activity unifying quantum information and condensed matter [1–5]. Entanglement quantifies the inseparability of quantum states. A separable state can be written as

$$\rho = \sum_i p_i \rho_A^i \otimes \rho_B^i, \tag{1}$$

where ρ_A^i and ρ_B^i are density matrices for the two subsystems A and $B = \bar{A}$, with probabilities $\sum_i p_i = 1$. Determining whether a mixed state is separable is NP-hard [6–8]. The criterion for a state to have finite negativity, i.e., negative eigenvalues after partial transposition, is a sufficient condition for inseparability [9–11].

In this paper we consider mixed states in the presence of a conserved charge, such as the total particle number $\hat{N} = \hat{N}_A + \hat{N}_B$, such that $[\rho, \hat{N}] = 0$. The separability condition Eq. (1) does not require that the individual classically combined components $\rho_A^i \otimes \rho_B^i$ are symmetric. Since the latter should describe plausible physical states, we supplement Eq. (1) by the symmetry condition

$$\forall_i \quad \left[\rho_A^i \otimes \rho_B^i, \hat{N}\right] = 0. \tag{2}$$

As a familiar example, a state of free bosons hopping on a lattice at temperature T and chemical potential μ, $\rho = e^{-\beta(H-\mu N)}/Z$, where $\beta = T^{-1}$ is the inverse temperature and Z is the partition function, has a separable form in terms of coherent states [12]. But since coherent states are not number eigenstates, Eq. (2) is not satisfied. Thus while this state has zero negativity, it does not satisfy symmetric separability. As a consequence of symmetric inseparability, we will show that such a state must contain entanglement in specific charge sectors.

In this paper we explore a measurable quantity that provides a necessary condition for symmetric separability, Eqs. (1) and (2). We consider the entropy change due to an unselective measurement of the subsystem's charge:

$$\Delta S_m = S(\rho_m) - S(\rho), \tag{3}$$

where $\rho_m = \sum_{N_A} \Pi(N_A)\rho\Pi(N_A)$, $S(\rho) = -\mathrm{Tr}(\rho \ln \rho)$, and $\Pi(N_A)$ is a projector to a fixed number N_A of the subsystem. Equivalently, $\Delta S_m = S(\rho||\rho_m)$ is the relative entropy of charge coherence with respect to N_A [13]; we refer to ΔS_m as the number entanglement (NE).

We show that ΔS_m vanishes for symmetrically separable states, so that $\Delta S_m > 0$ implies that a state cannot be symmetrically separable. In systems with a fixed particle number, $\Delta S_m > 0$ may only occur when negativity is already present [see Fig. 1(a)]. As our main result, in the general case with fluctuating number of particles, we show that whenever $\Delta S_m > 0$, there exists some total charge-N block in the density matrix which is inseparable and has finite negativity [see Fig. 1(b)]. Then entanglement can be extracted via a projection to a total charge sector. Importantly, $\Delta S_m > 0$ may happen even in (nonsymmetrically) separable states. In these cases the only way to display separability is by violating the symmetry Eq. (2).

Similar to Bell's inequalities, an entanglement witness gives a yes or no answer to the separability condition. Remarkably, we find that ΔS_m is not only an entanglement witness in mixed states with a conserved particle number. It is also an entanglement monotone. An entanglement monotone is nonincreasing under local operations and classical communication (LOCC) [14]. Here, we show that the NE, ΔS_m, is nonincreasing under symmetric LOCC, which conserve the total charge. This gives a comparative meaning to the value of the NE, allowing an interpretation in terms of the number of Bell pairs in the charge sector.

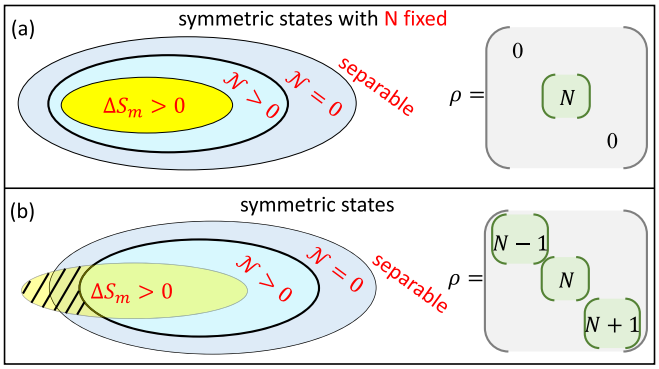

FIG. 1. The space of symmetric states ρ is divided by the thick ellipse into states with either finite or zero logarithmic negativity $\mathcal{N}$. Part of the latter are separable (white region). (a) For fixed particle number N, the set of states with finite ΔS_m (yellow region) is included in the set of states with finite negativity. (b) For general states with multiple total-charge blocks, describing, e.g., systems with a chemical potential, the set of states with finite ΔS_m may include separable states.

The paper is organized as follows. In Sec. II we describe the key properties of ΔS_m in general mixed states with a conserved charge. In Sec. III we show that ΔS_m is an entanglement monotone. In Sec. IV we connect ΔS_m with negativity, showing that whenever $\Delta S_m > 0$ there exists a charge sector with finite negativity; examples are given in Sec. V. In Sec. VI we describe methods to compute ΔS_m in extended one-dimensional (1D) systems, including numerical free-fermion methods, high-temperature expansion, and conformal field theory (CFT). We summarize in Sec. VII.

II. GENERAL PROPERTIES

Consider general symmetric mixed states ρ with $[\rho, \hat{N}] = 0$. To demonstrate that ΔS_m is a measure of symmetric inseparability, we note that ΔS_m satisfies a number of properties.

(1) $\Delta S_m \geqslant 0$.

(2) $\Delta S_m = 0$ for symmetric separable states.

One can show that $\Delta S_m \geqslant 0$ by demonstrating that ΔS_m equals the relative entropy between ρ and ρ_m [13,15]: $S(\rho||\rho_m) = \mathrm{Tr}(\rho \ln \rho) - \mathrm{Tr}(\rho \ln \rho_m)$. This follows from the fact that

$$\begin{aligned}\mathrm{Tr}(\rho_m \ln \rho_m) &= \sum_{N_A} \mathrm{Tr}[\Pi(N_A)\rho\Pi(N_A) \ln \rho_m] \\ &= \sum_{N_A} \mathrm{Tr}[\rho\Pi(N_A) \ln (\rho_m)\Pi(N_A)] \\ &= \mathrm{Tr}(\rho \ln \rho_m),\end{aligned}$$

where we used the property that ρ_m commutes with all projection operators $\Pi(N_A)$. So $\Delta S_m \geqslant 0$ follows directly from the positivity of the relative entropy.

To show that $\Delta S_m = 0$ for symmetrically separable states, satisfying Eqs. (1) and (2), let us temporarily focus on the simple product state, $\rho = \rho_A \otimes \rho_B$. The requirement $[\rho, \hat{N}] = 0$ implies $[\rho_A, \hat{N}_A] = 0$ (by taking a partial trace on both sides of the equation). So ρ_A actually commutes with all projection operators $\Pi(N_A)$. Thus the postmeasurement state is the same as ρ and there is no entropy change. The same is true for general symmetric-separable states since each component satisfies Eq. (2).

(3) ΔS_m is invariant under symmetry-preserving local unitary transformations. Here we consider local unitaries which preserve the total charge N. Because it is a local operator acting in either A or B, it preserves N_A, i.e., $[U, \hat{N}_A] = 0$. These could be unitaries acting on internal degrees of freedom. Then it is not hard to show that

$$\begin{aligned}\Delta S_m \to S\left[\sum_{N_A} \Pi(N_A) U\rho U^\dagger \Pi(N_A)\right] - S(U\rho U^\dagger) \\ = S\left[\sum_{N_A} \Pi(N_A)\rho\Pi(N_A)\right] - S(\rho) = \Delta S_m, \qquad (4)\end{aligned}$$

where we used the properties $S(\rho) = S(U\rho U^\dagger)$ and $[\Pi(N_A), U] = 0$, which follows from $[U, \hat{N}_A] = 0$.

(4) ΔS_m is symmetric if we exchange A and B. In other words if we choose to measure the particle number in B or in A, the postmeasurement states are the same, as obtained by annihilating all off-diagonal blocks with respect to N_A.

(5) ΔS_m is additive. Consider two flavors of particles $\rho = \rho^{f_1} \otimes \rho^{f_2}$. Here we require that the number of particles of each flavor N_{f_1} and N_{f_2} are separately conserved. Now if we separately measure the particle number of both flavors of particles in subsystem A, it is straightforward to show that $\rho_m = \rho_{f_1,m} \otimes \rho_{f_2,m}$ and hence $\Delta S_m(\rho) = S_m(\rho^{f_1}) + S_m(\rho^{f_2})$.

Pure states

We now study S_m in pure states. The most general pure state with N particles can be written as

$$|\Psi\rangle = \sum_{N_A} \sqrt{P(N_A)}\left(\sum_{i,\alpha} c_{i,\alpha}^{(N_A)} |N_A, i\rangle_A |N - N_A, \alpha\rangle_B\right), \qquad (5)$$

where $P(N_A)$ is the probability to find the subsystem A with charge N_A, i and α denote basis states in regions A and B for a given number of particles, and $c_{i,\alpha}^{(N_A)}$ are normalized as $\sum_{i,\alpha} |c_{i,\alpha}^{(N_A)}|^2 = 1$. For pure states obviously $S(\rho) = 0$, and

$$\Delta S_m = S(\rho_m) = -\sum_{N_A} P(N_A) \ln P(N_A) \ \text{(pure states)}. \qquad (6)$$

Thus, ΔS_m coincides for pure states with the number entropy [16–22], i.e., the entropy of the distribution function of the subsystem's charge. If one of the subsystems contains only one site (with no additional internal degrees of freedom) then the number entropy equals the entanglement entropy (EE) $S_{\mathrm{EE}} = S(\rho_A)$ where $\rho_A = \mathrm{Tr}_B \rho$, but in general $S_{\mathrm{EE}} > -\sum_{N_A} P(N_A) \ln P(N_A)$. In addition we note that the number entropy is bounded from above by $\ln(1 + N_{A,\max} - N_{A,\min})$ where $1 + N_{A,\max} - N_{A,\min}$ is the number of subsystem charge states. The part of the entanglement entropy not included in the number entropy is often referred to as configuration or accessible entropy [23–25], and it admits a symmetry resolution [16,17,19,26–36] (see Appendix A).

The relationship between ΔS_m, entanglement, and number entropy can be visualized by simple examples. Consider the state $|\Psi\rangle = \alpha\,|01\rangle + \beta\,|10\rangle$, defined on two sites, where $|0\rangle$ represents an empty site and $|1\rangle$ represents a filled site, with $|\alpha|^2 + |\beta|^2 = 1$. The reduced density matrix of the first site is $\rho_A = |\alpha|^2\,|0\rangle\langle 0| + |\beta|^2\,|1\rangle\langle 1|$. Consider measuring the particle number in the first site, yielding

$$\rho_m = |\alpha|^2\,|01\rangle\langle 01| + |\beta|^2\,|10\rangle\langle 10|\,. \tag{7}$$

In this example where the subsystem consists of a single site, N_A fully specifies the quantum state in A, and hence the entropy change coincides with the entanglement entropy and number entropy.

Now consider the following state on four sites:

$$|\Phi\rangle = \frac{1}{\sqrt{2}}(|0101\rangle + |1010\rangle), \tag{8}$$

which is entangled, and satisfies $[\hat{N}, |\Phi\rangle\langle\Phi|] = 0$. Consider measuring the particle number in the first two sites. In this case the quantum state does not change, i.e., $\Delta S_m = 0$. Similarly the number entropy vanishes. This example illustrates that ΔS_m does not capture the full entanglement, only the entanglement between different symmetry sectors.

However, in general mixed states the number entropy is unrelated to entanglement. This can be seen by the following example of a symmetrically separable (and hence unentangled) state:

$$\rho = \sum_{N_A} P(N_A)|N_A\rangle_A\langle N_A| \otimes |N - N_A\rangle_B\langle N - N_A|. \tag{9}$$

Now consider instead the following state on two sites:

$$|\phi\rangle = |0\rangle \otimes \frac{|0\rangle + |1\rangle}{\sqrt{2}}, \tag{10}$$

which is clearly a product state, with no entanglement. However, if we measure the particle number in the second site, the measured state is

$$\rho_m = |0\rangle\langle 0| \otimes \tfrac{1}{2}(|0\rangle\langle 0| + |1\rangle\langle 1|), \tag{11}$$

and the entropy change is not zero. ΔS_m fails to indicate entanglement here because $[\hat{N}, |\phi\rangle\langle\phi|] \neq 0$. This example illustrates that we have to restrict to those states which possess a conserved quantity.

III. MONOTONICITY

The discussion so far emphasized, through properties 1–5 listed in Sec. II, that the NE $\Delta S_m > 0$ is a witness of symmetric inseparability in mixed states with a conserved charge. Yet, the actual value of ΔS_m did not play any role. Now we provide a comparative meaning to the value of ΔS_m in different states, showing that ΔS_m is actually an entanglement monotone in the presence of charge conservation. We apply the results of Ref. [13] which made related claims.

To show that the NE is an entanglement monotone, we consider symmetric LOCC transformations:

$$\mathcal{K}(\rho) = \sum_n K_n \rho K_n^\dagger, \tag{12}$$

where the Lindblad operators K_n (i) satisfy [14] $\sum_n K_n^\dagger K_n = I$, (ii) can be written as $K_n = K_n^{(A)} \otimes K_n^{(B)}$, and (iii) satisfy the symmetry condition $[K_n, \hat{N}] = 0$. This goes beyond unitary transformations, as it describes coupling to a bath, and also includes classical communication. We will show that

$$\Delta S_m \text{ does not increase under symmetric LOCC.}$$

Thus the only way to increase ΔS_m is by genuine quantum entangling nonlocal operations. We demand the symmetry which is required for ΔS_m to be served as a witness of inseparability.

Proof. The NE is defined as the relative entropy of the unmeasured and measured states:

$$\Delta S_m(\rho) = \mathrm{Tr}[\rho \ln \rho] - \mathrm{Tr}\left[\rho \ln \sum_{N_A} \Pi(N_A)\rho\Pi(N_A)\right]. \tag{13}$$

We then need to prove that

$$\Delta S_m(\rho) \geqslant \Delta S_m(\mathcal{K}(\rho)), \tag{14}$$

where

$$\Delta S_m(\mathcal{K}(\rho)) = \mathrm{Tr}[\mathcal{K}(\rho)\ln\mathcal{K}(\rho)] - \mathrm{Tr}[\mathcal{K}(\rho)\ln\sum_{N_A}\Pi(N_A)\mathcal{K}(\rho)\Pi(N_A)]. \tag{15}$$

We proceed by showing that the symmetric LOCC transformation commutes with the charge measurement, namely,

$$\sum_{N_A} \Pi(N_A)\mathcal{K}(\rho)\Pi(N_A) = \mathcal{K}\left[\sum_{N_A}\Pi(N_A)\rho\Pi(N_A)\right]. \tag{16}$$

To prove this, we first use an alternative representation of the postprojective measurement state:

$$\rho_m = \sum_{N_A}\Pi(N_A)\rho\Pi(N_A) = \int_{-\pi}^{\pi}\frac{d\alpha}{2\pi}e^{i\alpha\hat{N}_A}\rho e^{-i\alpha\hat{N}_A}. \tag{17}$$

Notice that $\int_{-\pi}^{\pi}\frac{d\alpha}{2\pi}e^{i\alpha\hat{N}_A}\cdots e^{-i\alpha\hat{N}_A}$ acts as a projection operator, because $\int_{-\pi}^{\pi}\frac{dq}{2\pi}e^{iqN} = \delta_{N,0}$. In other words, it kills coherence between states with different N_A. We also use the properties of the symmetric LOCC operators K_n. As shown in Ref. [13], the K_n operators satisfy

$$[K_n, \hat{N}_A] = \delta_n K_n. \tag{18}$$

We then say that the Lindblad operator K_n has subsystem charge δ_n.

Using Eqs. (17) and (18), we have

$$\sum_{N_A}\Pi(N_A)\mathcal{K}(\rho)\Pi(N_A) = \sum_n\int_{-\pi}^{\pi}\frac{d\alpha}{2\pi}e^{i\alpha\hat{N}_A}K_n\rho K_n^\dagger e^{-i\alpha\hat{N}_A} = \sum_n\int_{-\pi}^{\pi}\frac{d\alpha}{2\pi}K_n e^{i\alpha\hat{N}_A}\rho e^{-i\alpha\hat{N}_A}K_n^\dagger = \mathcal{K}(\rho_m). \tag{19}$$

As a result of Eq. (16), we see that the entropy change after the symmetric LOCC becomes $\Delta S_m(\mathcal{K}(\rho)) = S(\mathcal{K}(\rho)||\mathcal{K}(\rho_m))$. Finally, we use a property of the relative entropy between two arbitrary density matrices $S(\rho||\sigma)$, being

nonincreasing under any completely positive trace preserving map applied on both ρ and σ [15]:

$$S(\rho||\sigma) \geqslant S[\mathcal{K}(\rho)||\mathcal{K}(\sigma)]. \tag{20}$$

This proves the monotonicity condition Eq. (14) [14].

We now discuss simple examples on two sites. First consider an initial product state $|00\rangle$ which is transformed via a local operation on the second site to the state $|\phi\rangle$ in Eq. (8). Under this LOCC ΔS_m increases. But as explained above $|\phi\rangle$ does not commute with the symmetry, and then ΔS_m does not measure entanglement. This example emphasizes that ΔS_m cannot increase under the specific LOCC transformations that conserve charge, and explains why this nonincreasing condition is restricted to symmetric LOCC.

As a second example, we consider a transformation that acts nontrivially only in the $N = 1$ sector, taking

$$|01\rangle\langle 01| \to \tfrac{1}{2}(|01\rangle\langle 01| + |10\rangle\langle 10|) \tag{21}$$

and

$$|10\rangle\langle 10| \to \tfrac{1}{2}(|01\rangle\langle 01| + |10\rangle\langle 10|). \tag{22}$$

This is an example of classical communication creating classical correlations between A and B but no entanglement. The Lindblad operators describing this process are

$$K_1 = \frac{1}{\sqrt{2}}|10\rangle\langle 10|, \quad K_2 = \frac{1}{\sqrt{2}}|01\rangle\langle 01|,$$
$$K_3 = \frac{1}{\sqrt{2}}|10\rangle\langle 01|, \quad K_4 = \frac{1}{\sqrt{2}}|01\rangle\langle 10|. \tag{23}$$

These operators satisfy conditions (i), (ii), and (iii). Consider an initial density matrix:

$$\rho = a|10\rangle\langle 10| + (1-a)|01\rangle\langle 01| + b|10\rangle\langle 01| + b^*|01\rangle\langle 10|, \tag{24}$$

the NE of which $\Delta S_m(\rho) > 0$ since it has a finite subsystem charge coherence $|b| \neq 0$. Now consider $\mathcal{K}(\rho)$:

$$\mathcal{K}(\rho) = \sum_n K_n \rho K_n^\dagger = \tfrac{1}{2}|10\rangle\langle 10| + \tfrac{1}{2}|01\rangle\langle 01|. \tag{25}$$

In this case, $\Delta S_m(\mathcal{K}(\rho)) = 0$, which satisfies Eq. (14).

IV. RELATION BETWEEN ΔS_m AND NEGATIVITY

Having demonstrated that ΔS_m witnesses symmetric inseparability, we now discuss its relation to negativity. Consider mixed states with a fixed number of particles, N. Logarithmic negativity is defined by $\mathcal{N} = \ln||\rho^{T_A}||$ where ^{T_A} represents a partial transposition with respect to subsystem A. We make two statements.

(1) If subsystem A has only one site, i.e., its state is fully specified by N_A, then the set of states with zero negativity equals the set of states with zero ΔS_m.

(2) If subsystem A contains more than one site, the set of states with zero negativity is included in the set of states with zero ΔS_m.

The second more general statement is illustrated in Fig. 1(a) and is proven as follows. The most general mixed

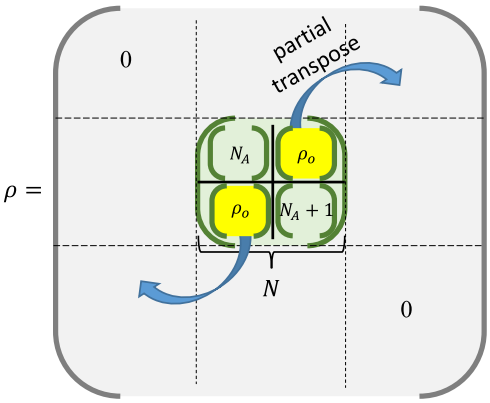

FIG. 2. The total charge-N block of the density matrix contains both diagonal and off-diagonal subblocks in terms of the subsystems charge N_A. Under partial transposition the off-diagonal blocks map to different total charge sectors [see Eq. (27)]. Under unselective measurement $\rho \to \rho_m$, the off-diagonal blocks are annihilated.

state with a fixed total particle number can be written as

$$\rho = \sum_{N_A,N_A',i,i',\alpha,\alpha'} C_{i,i',\alpha,\alpha'}^{N_A,N_A'} \times |N_A, i\rangle_A\langle N_A', i'| \otimes |N - N_A, \alpha\rangle_B\langle N - N_A', \alpha'|. \tag{26}$$

By considering separately terms in the sum with $N_A = N_A'$ and $N_A \neq N_A'$, we split the density matrix into two parts $\rho = \rho_d + \rho_o$, being either diagonal or off-diagonal with respect to N_A, respectively (see Fig. 2). If we perform a partial transposition with respect to A we obtain

$$\rho_d^{T_A} = \sum_{N_A,i,i',\alpha,\alpha'} C_{i,i',\alpha,\alpha'}^{N_A,N_A} \times |N_A, i'\rangle_A\langle N_A, i| \otimes |N - N_A, \alpha\rangle_B\langle N - N_A, \alpha'|,$$
$$\rho_o^{T_A} = \sum_{N_A\neq N_A',i,i',\alpha,\alpha'} C_{i,i',\alpha,\alpha'}^{N_A,N_A'} \times |N_A', i'\rangle_A\langle N_A, i| \otimes |N - N_A, \alpha\rangle_B\langle N - N_A', \alpha'|. \tag{27}$$

From these expressions it is clear that (i) $\rho_d^{T_A}$ still lies in the same symmetry sector with total particle number N, whereas on the other hand $\rho_o^{T_A}$ lies completely outside of the original symmetry sector (see Fig. 2); (ii) both $\rho_d^{T_A}$ and $\rho_o^{T_A}$ are Hermitian matrices because partial transposition preserves Hermiticity; and (iii) $\mathrm{Tr}\rho_o^{T_A} = 0$.

Because $\rho_d^{T_A}$ and $\rho_o^{T_A}$ lie in completely different sectors we can diagonalize them separately. The matrix $\rho_o^{T_A}$ is traceless and Hermitian. Thus all of its eigenvalues are real and sum up to zero. Hence negative eigenvalues are guaranteed unless all the eigenvalues vanish, i.e., all the matrix elements vanish.

Therefore, zero negativity means at least that ρ_o vanishes. The inverse is not true because some residue of the effect of partial transposition is acting on the internal i degrees of freedom. However, if there are no other degrees of freedom besides the local particle number in subsystem A, e.g., if it contains only one site, then the set of states with zero negativity equals the set of states with no off-diagonal elements with respect to N_A.

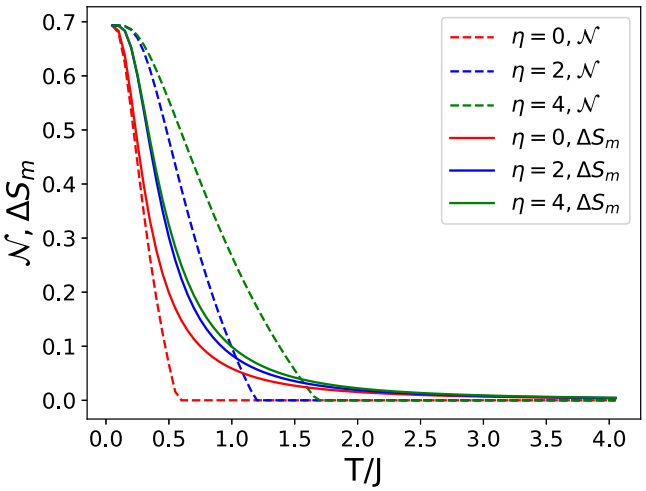

FIG. 3. Entropy change ΔS_m and logarithmic negativity $\mathcal{N}$ for the two-site XXZ model Eq. (28). The leftmost, middle, and rightmost solid (dashed) lines correspond to ΔS_m ($\mathcal{N}$) for $\eta = 0, 2, 4$, respectively. While the latter displays a sudden death above some interaction dependent temperature [37], we have $\Delta S_m > 0$ indicating finite entanglement in fixed sectors at any temperature.

Now consider mixed states with fluctuating total N as in Fig. 1(b). From statement 2 above we deduce our main statement: *If a symmetric state has $\Delta S_m > 0$ then it necessarily contains negativity in some charge sectors.* Thus, entanglement can be extracted by projection to a fixed total charge sector. This statement follows because $\Delta S_m > 0$ ensures that there exists at least one charge-N block with finite ρ_o.

The generalization of the concept of negativity based on partial transposition to fermionic systems had been a challenge addressed recently [38–40]. In Appendix C we comment on the comparison of ΔS_m and fermionic negativity.

V. EXAMPLES

A. Sudden death of entanglement in the XXZ model

We now consider an example illustrating that $\Delta S_m > 0$ implies entanglement in fixed charge sectors even when $\mathcal{N} = 0$. As a standard interacting model with a U(1) symmetry, consider the XXZ Hamiltonian

$$H_{XXZ} = J \sum_{i=1}^{L-1} \left(s_i^x s_{i+1}^x + s_i^y s_{i+1}^y + \eta s_i^z s_{i+1}^z \right), \tag{28}$$

where s_i^a are spin-1/2 operators acting on site i. This 1D model is equivalent to interacting hard-core bosons, or fermions, with hopping amplitude $t = \frac{J}{2}$ and interaction $J\eta$. s^z conservation maps to a particle number conservation. The thermal state $\rho = \frac{e^{-\beta H_{XXZ}}}{Z}$ was shown [37] to display a sudden death of negativity at some critical temperature. However, we find that $\Delta S_m > 0$ at any temperature. The comparison of $\mathcal{N}$ and ΔS_m is plotted in Fig. 3 in the simple case with $L = 2$ and $L_A = 1$. The thermal density matrix can be written as

$$\rho = \frac{1}{Z} \begin{array}{c} \begin{matrix} |00\rangle & |01\rangle & |10\rangle & |11\rangle \end{matrix} \\ \begin{pmatrix} e^{-\frac{\beta\eta}{4}} & 0 & 0 & 0 \\ 0 & e^{\frac{\beta\eta}{4}} \cosh\frac{\beta}{2} & -e^{\frac{\beta\eta}{4}} \sinh\frac{\beta}{2} & 0 \\ 0 & -e^{\frac{\beta\eta}{4}} \sinh\frac{\beta}{2} & e^{\frac{\beta\eta}{4}} \cosh\frac{\beta}{2} & 0 \\ 0 & 0 & 0 & e^{-\frac{\beta\eta}{4}} \end{pmatrix} \end{array}.$$

We can see that there is entanglement in the $N = 1$ sector, which is encoded in the off-diagonal elements $\propto \sinh(\beta/2)$. A similar situation occurs for thermal free bosons as discussed in Appendix B. Extending on this example, we now construct examples of separable states with $\Delta S_m > 0$, either for bosons or for fermions.

B. Separable states with $\Delta S_m > 0$

We now provide two examples of separable states with $\Delta S_m > 0$, as marked with diagonal lines in Fig. 1(b). Although these states are separable they contain entanglement in specific charge sectors. The only way to achieve a separable form is by violating Eq. (2) on the level of each classically combined component.

1. Two-site spin state

As an example illustrating that $\Delta S_m > 0$ implies entanglement in fixed charge sectors even for separable states, consider the two-site example

$$\begin{aligned} \rho = \tfrac{1}{4}(&|x_+\rangle\langle x_+| \otimes |x_-\rangle\langle x_-| + |x_-\rangle\langle x_-| \otimes |x_+\rangle\langle x_+| \\ &+ |y_+\rangle\langle y_+| \otimes |y_-\rangle\langle y_-| + |y_-\rangle\langle y_-| \otimes |y_+\rangle\langle y_+|), \end{aligned} \tag{29}$$

where $|x_\pm\rangle$ and $|y_\pm\rangle$ are states with ± 1 eigenvalues of the Pauli-matrix operators σ^x and σ^y, respectively. Mapping spin $\uparrow$ ($\downarrow$) to an occupied (empty) site, we use the basis $\{|00\rangle, |01\rangle, |10\rangle, |11\rangle\}$. This state can be written as $\rho = \frac{1}{4}(|00\rangle\langle 00| + |11\rangle\langle 11|) + \frac{1}{2}|\psi_-\rangle\langle\psi_-|$, where $|\psi_-\rangle = \frac{|01\rangle - |10\rangle}{\sqrt{2}}$. We see that this explicitly separable state has a block structure, i.e., $[\rho, \hat{N}] = 0$. Clearly, this state has $\Delta S_m > 0$ and it indeed has a nonseparable charge sector of $N = 1$. Neither of the components of Eq. (29) conserves the symmetry; only their sum does.

2. Fermions

In dealing with fermionic systems we first deal with parity conservation. Separable states are defined as in Eq. (1) where, importantly, we require

$$\left[\rho_A^i, (-1)^{N_A}\right] = 0. \tag{30}$$

We divide nonseparable states into two branches [39]: (1) states with a block-diagonal form in terms of the fermion-number parity of the subsystem,

$$[\rho, (-1)^{F_A}] = 0, \tag{31}$$

and (2) states containing off-diagonal blocks in terms of the fermion-number parity of the subsystem,

$$[\rho, (-1)^{F_A}] \neq 0. \tag{32}$$

It is clear that $\Delta S_m^{(\text{parity})}$, the entropy change induced by a parity measurement, is nonzero for all nonseparable states in branch 2.

Now, suppose that besides the fermion-number parity, we have an additional U(1) symmetry. As in the bosonic case, we could find separable states where each decomposition does not conserve this U(1) symmetry.

Analogous to the bosonic counterexample, consider the following mixed state of four fermions:

$$\rho = \begin{array}{c} \begin{matrix} |0000\rangle & |0011\rangle & |1100\rangle & |1111\rangle \end{matrix} \\ \begin{pmatrix} \frac{1}{4} & 0 & 0 & 0 \\ 0 & \frac{1}{4} & -\frac{1}{4} & 0 \\ 0 & -\frac{1}{4} & \frac{1}{4} & 0 \\ 0 & 0 & 0 & \frac{1}{4} \end{pmatrix} \end{array},$$

where the subsystem A consists of the first two sites. This mixed state has a decomposition similar to the mixed state of two qubits, while preserving the local fermion parity. This separable state has zero negativity, but has a finite ΔS_m. This state is of branch 1.

VI. CALCULATION METHODS AND SCALING PROPERTIES

We are now interested in the scaling of ΔS_m with T, L, and L_A. The von Neumann entropy ΔS_m can in principle be calculated from its Rényi moments via the replica trick using analytic methods [1]. Leaving this formidable task to future work, here we focus on the second moment of the NE, i.e., the change of second Rényi entropy $\Delta S_2 = S_2(\rho_m) - S_2(\rho)$, where $S_2 = -\ln \mathrm{Tr}\rho^2$.

According to Eq. (17), for a thermal state $\rho = \frac{e^{-\beta H}}{Z}$, we need to calculate

$$\mathrm{Tr}\rho_m^2 = \int \frac{d\alpha_1 d\alpha_2}{(2\pi)^2} \frac{1}{Z^2} \mathrm{Tr}(e^{-\beta H} e^{-i\alpha_{12}\hat{N}_A} e^{-\beta H} e^{i\alpha_{12}\hat{N}_A}), \quad (33)$$

where $\alpha_{12} = \alpha_1 - \alpha_2$.

We apply this formula as a starting point for various methods: (i) numerical calculation for free fermions, (ii) CFT, and (iii) high-temperature expansion. To illustrate these methods below, the model of interest is a free-fermion chain, $H = -t\sum_i (c_{i+1}^\dagger c_i + \text{H.c.})$.

A. Numerical results

We first develop a numerical method to calculate ΔS_2 (and similar quantities) in lattice models of free fermions. The method is based on properties of Gaussian operators. Specifically,

$$e^{c_i^\dagger A_{ij} c_j} e^{c_m^\dagger B_{mn} c_n} = e^{c_k^\dagger F_{kl} c_l}, \quad (34)$$

where $F = \ln(e^A e^B)$. This can be proven using the Baker-Campbell-Hausdorff formula. Secondly,

$$\mathrm{Tr} e^{c_i^\dagger S_{ij} c_j} = \det(\mathcal{I} + e^S). \quad (35)$$

This holds true for a general non-Hermitian S (see Ref. [41]). We start with Eq. (33). It is important to notice that both $e^{-\beta H}$ and $e^{-i(\alpha_1-\alpha_2)\hat{N}_A}$ are Gaussian operators. According to Eq. (34), the product of four Gaussian operators is still Gaussian, and the trace can be calculated using Eq. (35).

So suppose $H = \sum_{i,j} c_i^\dagger h_{ij} c_j$, and $\hat{N}_A = \sum_{i,j} c_i^\dagger n_{ij}^A c_j$. Then we conclude

$$\mathrm{Tr}(e^{-\beta H} e^{-i(\alpha_1-\alpha_2)\hat{N}_A} e^{-\beta H} e^{i(\alpha_1-\alpha_2)\hat{N}_A}) = \det(\mathcal{I} + e^{-\beta h} e^{-i\alpha_{12} n^A} e^{-\beta h} e^{i\alpha_{12} n^A}). \quad (36)$$

The calculation of Z in Eq. (33) and the second Rényi entropy of the unmeasured state $S_2(\rho)$ is straightforward.

Using the above methods, we calculate ΔS_2 in a chain of size $L = 1000$; the subsystem size is fixed to be $L_A = 100$. We plot the temperature dependence of ΔS_2 in the right panel of Fig. 4, as square symbols.

B. High-temperature limit

At temperatures $T \gg t$, performing a high-temperature expansion we find that in a general lattice with hopping amplitude t and area $\mathcal{A}$ separating A and B, the NE becomes

$$\Delta S_m \to (t^2\mathcal{A})/(4T^2) \quad (37)$$

The derivation, which is essentially an expansion in β of Eq. (33), is given in Appendix D. This form holds true for the second Rényi entropy as shown in the inset of the right panel of Fig. 4.

C. CFT methods

To obtain the NE at $T = 0$, we borrow results for the number entropy [16,22] $\Delta S_m \sim \frac{1}{2}\ln(\frac{2K}{\pi}\ln L_A)$ where K is the Luttinger parameter. This is demonstrated in the left panel of Fig. 4 for noninteracting fermions, and also compared with the entanglement entropy S_{EE} [1]. While the two coincide for a single site in A, $S_{\text{EE}} \sim \frac{1}{3}\ln L_A$ exceeds ΔS_m, since the NE only captures entanglement between charge degrees of freedom.

We now are interested in the scaling of the NE at finite temperature, which is either small or large compared to the level spacing within the subsystem ($\propto 1/L_A$). Using CFT methods, we can express $\Delta S_2 = -\ln \frac{\mathrm{Tr}\rho_m^2}{\mathrm{Tr}\rho^2} = -\ln \int \frac{d\alpha_1 d\alpha_2}{(2\pi)^2} V_1 V_2 V_3 V_4{}_{2\beta}$ in terms of a correlation function on a cylinder of circumference 2β, with $V_1 V_2 V_3 V_4{}_{2\beta} = (\frac{2\beta}{\pi}\tanh\frac{\pi L_A}{2\beta})^{-\frac{(\alpha_1-\alpha_2)^2}{\pi^2}}$. The details of the derivation are given in Appendix E. This is valid for any ratio β/L_A, as long as T is lower than the high-energy cutoff Λ, set by t. From this, we derive a crossover from the low-temperature regime discussed above, to an intermediate-temperature regime, $\frac{1}{L_A} \ll T \ll \Lambda$, where we find $\Delta S_2 \sim \frac{1}{2}\ln\ln\beta$. This is compared with numerical results in the right panel of Fig. 4. Deviations from CFT results are seen for $T \lesssim \Lambda$.

The result for the NE combining these various methods is summarized in the central panel of Fig. 4. We can see that at zero temperature the NE coincides with the number entropy, which itself is only a part of the entanglement entropy, except when the subsystem has only one site. The definition of the NE ΔS_m extends to finite temperature, where at very high temperature it decays as $1/T^2$ according to an area law.

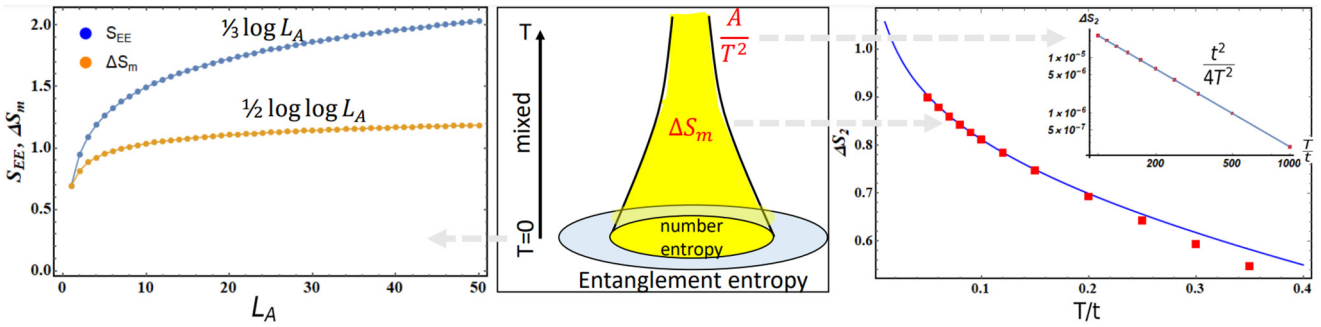

FIG. 4. Middle panel: Schematic temperature dependence of ΔS_m for general systems. At $T \to 0$ it approaches the number entropy, which is contained in the entanglement entropy $S_{\rm EE}$. At high temperature it decays as $1/T^2$ following an area law. Left panel: Comparison of $S_{\rm EE}$ (upper) and ΔS_m (lower) at $T = 0$ for free fermions and $L \to \infty$, L_A denotes the number of sites in subsystem A. Analytic fits are $\Delta S_m \cong \frac{1}{2}\ln[1.731(\ln L_A + 2.269)]$ and $S_{\rm EE} \cong \frac{1}{3}\ln L_A + .726$. Right panel: Second Rényi entropy ΔS_2 for $L = 1000$ and $L_A = 100$ using numerical (squares) and CFT results. Inset: Fit to $1/T^2$ form.

VII. SUMMARY

A projective measurement the result of which is not being recorded increases the entropy of a quantum system. When applied to a subsystem in a conserved charge basis, it annihilates any coherences between blocks with different subsystem charges. The entropy change, referred to as number entanglement, indicates entanglement, or inseparability between the measured subsystem and its complement.

The NE quantifies entanglement in mixed states as long as the density matrix commutes with the symmetry. It goes beyond other quantities such as entanglement entropy, which is restricted to pure states, or logarithmic negativity, which does not account for the symmetry resolution of inseparability.

There are a number of directions to measure ΔS_m in experiment. These include cold atom experiments realizing the replica trick [42], which also allow one to measure negativity [26,43], as well as experiments realizing random unitaries [33,44]. Another promising direction is based on mesoscopic systems. Recently, it was demonstrated how to measure changes of entropy [45–48]. We envision ΔS_m as a special case of an entropy change occurring as we turn on a nearby mesoscopic conductor acting as charge detector, which causes dephasing and decoherence [49,50].

ACKNOWLEDGMENTS

We acknowledge support from the European Research Council under the European Unions Horizon 2020 research and innovation program under Grant No. 951541, U.S. Army Research Office Grant No. W911NF-20-1-0013, U.S.-Israel Binational Science Foundation Grant No. 2016255, and Israel Science Foundation Grant No. 154/19. We thank Pasquale Calabrese, Marcello Dalmonte, Moshe Goldstein, and Tarun Grover for discussions.

APPENDIX A: RELATION TO SYMMETRY-RESOLVED ENTANGLEMENT

In this Appendix, we discuss the entropy change upon measurement, ΔS_m, in the context of entanglement entropy and symmetry-resolved entanglement (SRE).

For pure states with a global conserved charge the entanglement entropy can be separated as

$$S(\rho_A) = H_1\{[P(N_A)]\} + \sum_{N_A} P(N_A) S[\rho_A(N_A)], \qquad (T = 0). \tag{A1}$$

Here $H_1\{[P(N_A)]\} = -\sum_{N_A} P(N_A)\ln P(N_A)$ is the Shannon entropy of the subsystem charge probability distribution, which we refer to as number entropy. Also it is often referred to as inaccessible entanglement [24,25]. The second term [23] is the weighted contribution of the SRE originating from each superselection sector corresponding to N_A particles in A, where

$$\rho_A(N_A) = \frac{1}{P(N_A)}\Pi(N_A)\rho_A\Pi(N_A). \tag{A2}$$

This separation of the EE into a number entropy and the weighted SRE is displayed in Fig. 4 of the main text. Relatedly, connections between entanglement entropy and charge fluctuations were emphasized in one dimension [51–53].

In this paper we consider a general mixed density matrix ρ and our quantity of interest is

$$\Delta S_m = H_1\{[P(N_A)]\} + \sum_{N_A} P(N_A)\{S[\rho(N_A)] - S(\rho)\}. \tag{A3}$$

Here, compared to the pure state decomposition Eq. (A1), in the second term we have the entropy of the full state acting both on A and on B after it has been projected and normalized to a given number of particles in A:

$$\rho(N_A) = \frac{1}{P(N_A)}\Pi(N_A)\rho\Pi(N_A). \tag{A4}$$

Note the difference compared to Eq. (A2) which involves the reduced density matrix. Thus the second term in Eq. (A3) is the weighted entropy change for each charge state. Interestingly, this is equivalent to our simple definition Eq. (3). Note that in Eq. (3) $\rho_m = \sum_{N_A}\Pi(N_A)\rho\Pi(N_A) = \oplus_{N_A} P(N_A)\rho(N_A)$ is normalized but consists of non-normalized blocks.

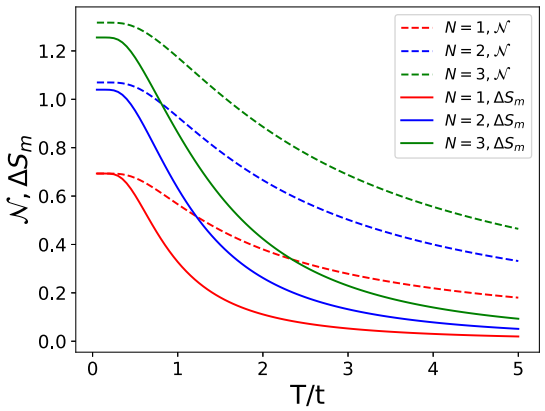

FIG. 5. The uppermost, middle, and lowermost solid (dashed) lines correspond to ΔS_m ($\mathcal{N}$) for $N = 3, 2, 1$, respectively.

APPENDIX B: THERMAL STATE OF TWO BOSON MODES

We consider the Hamiltonian

$$H = (a_1^\dagger \quad a_2^\dagger)\begin{pmatrix} -\mu & t \\ t & -\mu \end{pmatrix}\begin{pmatrix} a_1 \\ a_2 \end{pmatrix},$$

which conserves the total particle number N. The Gibbs state $\rho = e^{-\beta H}$ was shown to be separable [12]. Hence the negativity of the full state vanishes.

However, according to our results, some of the symmetry sectors $\rho(N) = \Pi(N)\rho\Pi(N)$ are entangled, because the off-diagonal terms in N_A generally exist in the occupation number basis. In the following, we calculate ΔS_m and negativity in the $N = 1, 2, 3$ sectors, and plot both of them in Fig. 5.

The state we consider is $\rho = \frac{1}{Z}e^{-\beta H}\Pi(N)$, or equivalently $\rho = \frac{1}{Z}e^{-\beta H(N)}$ where $H(N)$ is the charge-N block of H.

In the one boson subspace, H can be written as

$$H_1 = \begin{array}{c} \quad |10\rangle \quad |01\rangle \\ \end{array}\begin{pmatrix} -\mu & t \\ t & -\mu \end{pmatrix}.$$

Thus we have

$$\rho = \frac{1}{Z}e^{-\beta H_1} = \begin{pmatrix} \frac{1}{2} & -\frac{1}{2}\tanh\beta \\ -\frac{1}{2}\tanh\beta & \frac{1}{2} \end{pmatrix}.$$

After simple algebra, we find that the negativity and the entropy change are

$$\mathcal{N} = \ln(1 + \tanh\beta), \tag{B1}$$

$$\Delta S_m = \ln 2 + \frac{1-\tanh\beta}{2}\ln\frac{1-\tanh\beta}{2} + \frac{1+\tanh\beta}{2}\ln\frac{1+\tanh\beta}{2}. \tag{B2}$$

Similarly we could derive the negativity and entropy change in $N = 2, 3$ subspaces, as plotted in Fig. 5.

APPENDIX C: FERMIONIC NEGATIVITY

In this Appendix we comment on the comparison of ΔS_m and fermionic negativity. The generalization of the concept of negativity based on partial transposition to fermionic systems had been a challenge addressed recently [38–40]. First, the example in Sec. V B 2 gives a fermionic state with ΔS_m, but zero fermionic negativity. In this sense, also the fermionic negativity fails to account for the additional U(1) symmetry that can allow one to extract entanglement by projecting to specific sectors. Below we show results for the fermionic negativity $\mathcal{N}^f$ and ΔS_m for the same XXZ two-site system studied in the main text. We first provide definitions. To define fermionic negativity, we first need to define fermionic partial transpose. In the occupation number basis,

$$|\{n_j\}_{j\in A}, \{n_j\}_{j\in B}\rangle = (f_{j_1}^\dagger)^{n_{j_1}} \cdots (f_{j_{m_A}}^\dagger)^{n_{j_{m_A}}} \cdots (f_{j'_{m_B}}^\dagger)^{n_{j'_{m_B}}} |0\rangle, \tag{C1}$$

the fermionic partial transpose is defined as

$$(|\{n_j\}_{j\in A}, \{n_j\}_{j\in B}\rangle \langle\{\bar{n}_j\}_{j\in A}, \{\bar{n}_j\}_{j\in B}|)^{R_A} = (-1)^{\phi(n_j,\bar{n}_j)} U_A^\dagger |\{\bar{n}_j\}_{j\in A}, \{n_j\}_{j\in B}\rangle \langle\{n_j\}_{j\in A}, \{\bar{n}_j\}_{j\in B}| U_A. \tag{C2}$$

To make a distinction between fermionic partial transpose and normal partial transpose, here we denote it as $(|\cdots\rangle\langle\cdots|)^{R_A}$. We can see it is the same as normal partial transpose up to a phase factor. Because of this phase factor, the fermionic partial transpose of a density matrix is no longer Hermitian. The fermionic negativity is defined as

$$\mathcal{N}^f = \ln \mathrm{Tr}\sqrt{\rho^{R_A}(\rho^{R_A})^\dagger}. \tag{C3}$$

As an explicit example, let us calculate the fermionic negativity in the XXZ model. Performing Jordan-Wigner transformation to the two-site XXZ Hamiltonian Eq. (28), we obtain

$$H = J\left[-\frac{1}{2}(c_1c_2^\dagger + c_2c_1^\dagger) + \eta(1-2c_1^\dagger c_1)(1-2c_2^\dagger c_2)\right]. \tag{C4}$$

The thermal density matrix $\rho = e^{-\beta H}/Z$ is

$$\rho = \frac{1}{Z}\begin{array}{c} \quad |00\rangle \quad |01\rangle \quad |10\rangle \quad |11\rangle \\ \end{array}\begin{pmatrix} e^{-\frac{\beta\eta}{4}} & 0 & 0 & 0 \\ 0 & e^{\frac{\beta\eta}{4}}\cosh\frac{\beta}{2} & -e^{\frac{\beta\eta}{4}}\sinh\frac{\beta}{2} & 0 \\ 0 & -e^{\frac{\beta\eta}{4}}\sinh\frac{\beta}{2} & e^{\frac{\beta\eta}{4}}\cosh\frac{\beta}{2} & 0 \\ 0 & 0 & 0 & e^{-\frac{\beta\eta}{4}} \end{pmatrix}. \tag{C5}$$

The fermionic partial transpose of ρ^{R_A} times Z is

$$\begin{array}{c} \quad |00\rangle \quad |01\rangle \quad |10\rangle \quad |11\rangle \\ \end{array}\begin{pmatrix} e^{-\frac{\beta\eta}{4}} & 0 & 0 & -ie^{\frac{\beta\eta}{4}}\sinh\frac{\beta}{2} \\ 0 & e^{\frac{\beta\eta}{4}}\cosh\frac{\beta}{2} & 0 & 0 \\ 0 & 0 & e^{\frac{\beta\eta}{4}}\cosh\frac{\beta}{2} & 0 \\ -ie^{\frac{\beta\eta}{4}}\sinh\frac{\beta}{2} & 0 & 0 & e^{-\frac{\beta\eta}{4}} \end{pmatrix}.$$

Then we could calculate $\mathcal{N}^f$, as in Eq. (C3). We plot the temperature and interaction strength dependence of $\mathcal{N}^f$ in Fig. 6.

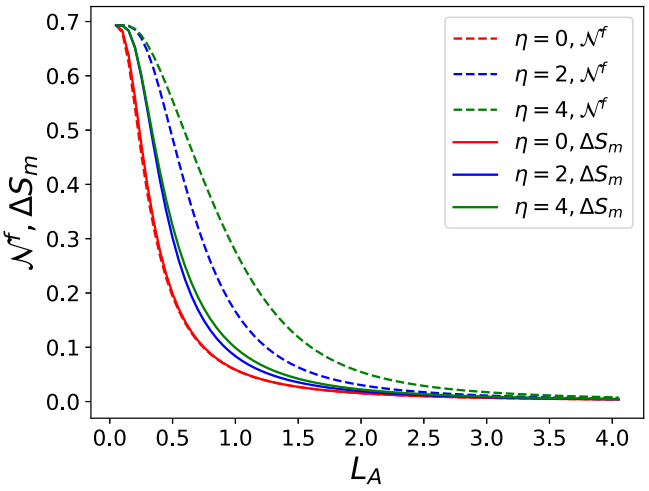

FIG. 6. $\mathcal{N}^f$ and ΔS_m of ρ in Eq. (C5); the leftmost, middle, and rightmost solid (dashed) lines correspond to ΔS_m ($\mathcal{N}^f$) for $\eta = 0, 2, 4$, respectively.

APPENDIX D: HIGH-TEMPERATURE EXPANSION

In this Appendix, we work out the high-temperature expansion of ΔS_2 and ΔS_m in the tight-binding chain of free fermions:

$$H = -t \sum_i (c_{i+1}^\dagger c_i + \text{H.c.}). \tag{D1}$$

The analysis below shows that it is sensitive to the hopping terms in the Hamiltonian, and immune to the interactions, as one might expect. According to Eq. (33),

$$\Delta S_2 = -\ln \int \frac{d\alpha_1 d\alpha_2}{(2\pi)^2} \frac{\text{Tr}(e^{-\beta H} e^{-i\alpha_{12}\hat{N}_A} e^{-\beta H} e^{i\alpha_{12}\hat{N}_A})}{\text{Tr} e^{-2\beta H}}. \tag{D2}$$

Here and in the following, $\alpha_{ij} = \alpha_i - \alpha_j$. For the denominator, we have the high-temperature expansion:

$$\begin{aligned} \text{Tr} e^{-2\beta H} &\approx \text{Tr}\left[\mathcal{I} - 2\beta H + \frac{(2\beta)^2}{2} H^2\right] \\ &= D_H - 2\beta \text{Tr} H + \frac{(2\beta)^2}{2} \text{Tr} H^2. \end{aligned} \tag{D3}$$

Clearly, D_H denotes the dimension of the Hilbert space. For the numerator, similarly we have

$$\begin{aligned} &\text{Tr}(e^{-\beta H} e^{-i\alpha_{12}\hat{N}_A} e^{-\beta H} e^{i\alpha_{12}\hat{N}_A}) \\ &\approx D_H - 2\beta \text{Tr} H + \beta^2 \text{Tr} H^2 \\ &+ \beta^2 \text{Tr}(H e^{-i\alpha_{12}\hat{N}_A} H e^{i\alpha_{12}\hat{N}_A}). \end{aligned} \tag{D4}$$

In the above expression, we used the cyclic property of the trace. Comparing Eqs. (D3) and (D4), we see that

$$\begin{aligned} &\frac{\text{Tr}(e^{-\beta H} e^{-i\alpha_{12}\hat{N}_A} e^{-\beta H} e^{i\alpha_{12}\hat{N}_A})}{\text{Tr} e^{-2\beta H}} \\ &\approx 1 + \beta^2 \frac{\text{Tr}(H e^{-i\alpha_{12}\hat{N}_A} H e^{i\alpha_{12}\hat{N}_A}) - \text{Tr} H^2}{D_H}. \end{aligned} \tag{D5}$$

From the above expression, we can infer that the lowest order of β expansion of ΔS_2 is the β^2 order. Equation (D5) can be simplified further:

$$\text{Tr}(H e^{-i\alpha_{12}\hat{N}_A} H e^{i\alpha_{12}\hat{N}_A}) - \text{Tr} H^2 = \text{Tr}(HO), \tag{D6}$$

where

$$O = e^{-i\alpha_{12}\hat{N}_A} H e^{i\alpha_{12}\hat{N}_A} - H. \tag{D7}$$

Most of the terms in H actually commute with $\hat{N}_A$, except for those terms that live at the boundary. Specifically, suppose that

$$\hat{N}_A = c_1^\dagger c_1 + \cdots + c_m^\dagger c_m, \tag{D8}$$

and that H is given by Eq. (D1). Here $m = L_A$ is the number of sites of subregion A. Then the only terms which have a nonvanishing commutator with $\hat{N}_A$, and thus contribute to O, are $H_{\text{hop}} = -t(c_0^\dagger c_1 + c_1^\dagger c_0 + c_m^\dagger c_{m+1} + c_{m+1}^\dagger c_m)$, which generate hopping of particles between A and its complement. The operator O can be calculated using the Baker-Campbell-Hausdorff formula:

$$\begin{aligned} &e^{-i\alpha_{12}\hat{N}_A} H e^{i\alpha_{12}\hat{N}_A} \\ &= H + i\alpha_{21}[\hat{N}_A, H] + \frac{(i\alpha_{21})^2}{2}[\hat{N}_A, [\hat{N}_A, H]] + \cdots. \end{aligned} \tag{D9}$$

Interestingly, we find

$$\begin{aligned} &[\hat{N}_A, H_{\text{hop}}] \\ &= -t(-c_0^\dagger c_1 + c_1^\dagger c_0 + c_m^\dagger c_{m+1} - c_{m+1}^\dagger c_m), \end{aligned} \tag{D10}$$

$$\begin{aligned} &[\hat{N}_A, [\hat{N}_A, H_{\text{hop}}]] \\ &= -t(c_0^\dagger c_1 + c_1^\dagger c_0 + c_m^\dagger c_{m+1} + c_{m+1}^\dagger c_m) = H_{\text{hop}}. \end{aligned} \tag{D11}$$

Then Eq. (D9) yields

$$\begin{aligned} &e^{-i\alpha_{12}\hat{N}_A} H_{\text{hop}} e^{i\alpha_{12}\hat{N}_A} \\ &= \cos\alpha_{21} H_{\text{hop}} + i \sin\alpha_{21}[\hat{N}_A, H_{\text{hop}}]. \end{aligned} \tag{D12}$$

So we conclude

$$O = \cos\alpha_{21} H_{\text{hop}} + i \sin\alpha_{21}[\hat{N}_A, H_{\text{hop}}] - H_{\text{hop}}. \tag{D13}$$

To calculate $\text{Tr}(HO)$, notice that

$$\text{Tr} c_i^\dagger c_j = \tfrac{1}{2}\delta_{ij} D_H, \tag{D14}$$

$$\text{Tr} c_i^\dagger c_j c_m^\dagger c_n = \tfrac{1}{4}(\delta_{ij}\delta_{mn} + \delta_{in}\delta_{mj}) D_H. \tag{D15}$$

The only part in H which contributes to $\text{Tr}(HO)$ is H_{hop} again. Then

$$\begin{aligned} \text{Tr}(HO) &= (\cos\alpha_{21} - 1)\text{Tr} H_{\text{hop}}^2 \\ &+ i \sin\alpha_{21} \text{Tr}(H_{\text{hop}}[\hat{N}_A, H_{\text{hop}}]). \end{aligned} \tag{D16}$$

After integration over α_2 and α_1, we conclude

$$\Delta S_2 = -\ln\left(1 - \beta^2 \frac{\text{Tr} H_{\text{hop}}^2}{D_H}\right) \approx \beta^2 \frac{\text{Tr} H_{\text{hop}}^2}{D_H} = \beta^2 t^2. \tag{D17}$$

This result holds when $\beta^2 t^2 \ll 1$. For a general lattice in any dimension, with nearest-neighbor hopping, we have

$$\Delta S_2 = \frac{\mathcal{A} t^2}{2T^2}, \tag{D18}$$

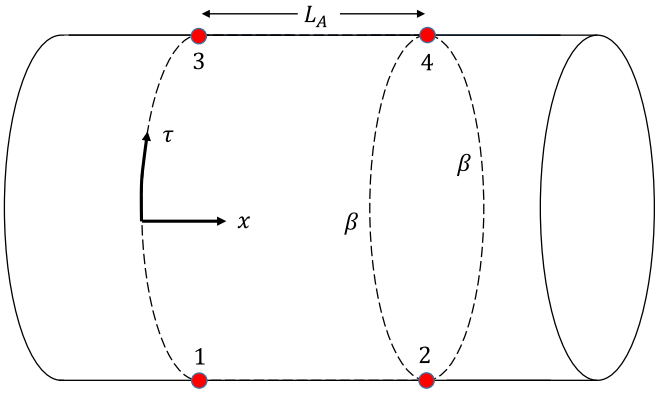

FIG. 7. Cylinder geometry of circumference 2β where the correlation function $V_1V_2V_3V_4$ is computed.

where the hopping amplitude t is assumed to be constant and $\mathcal{A}$ is the area between A and B. For our 1D case, we have $\mathcal{A} = 2$. Now consider a fermion chain with nearest-neighbor interactions:

$$H = -t\sum_i (c_{i+1}^\dagger c_i + c_i^\dagger c_{i+1}) + V\sum_i n_i n_{i+1}. \tag{D19}$$

This Hamiltonian also preserves the total particle number. Although there might exist strong interaction between the fermions, the above analysis yields the same high-temperature expansion of ΔS_2. Specifically notice that $[\hat{N}_A, n_i n_{i+1}] = 0$ for all i. Essentially the same analysis leads to the high-temperature expansion of ΔS_m, defined as

$$\begin{aligned}\Delta S_m &= S(\rho_m) - S(\rho)\\ &= -\lim_{n\to 1}\partial_n \mathrm{Tr}\rho_m^n - (-\lim_{n\to 1}\partial_n \mathrm{Tr}\rho^n).\end{aligned} \tag{D20}$$

The high-temperature expansion turns out to be

$$\Delta S_m = \tfrac{1}{2}(\beta t)^2. \tag{D21}$$

This result is also immune to the interaction. A similar result has been derived for the mutual information [54].

APPENDIX E: CFT METHODS

In the following, we identify the trace in Eq. (33) as a path integral on a cylinder of circumference 2β with angular variable τ and infinite coordinate x (see Fig. 7). Following a related computation of the SRE [16], each of the operators $e^{\pm i\alpha\hat{N}_A}$ at $\tau = 0$ and $\tau = \beta$ is realized by a pair of vertex operator insertions as $e^{i\alpha\hat{N}_A} = e^{i\frac{\alpha}{2\pi}\phi(\tau,L_A)}e^{-i\frac{\alpha}{2\pi}\phi(\tau,0)}$. We obtain a normalized correlation function of vertex operators:

$$\frac{\mathrm{Tr}(e^{-\beta H}e^{-i(\alpha_1-\alpha_2)\hat{N}_A}e^{-\beta H}e^{i(\alpha_1-\alpha_2)\hat{N}_A})}{\mathrm{Tr}e^{-2\beta H}} = V_1V_2V_3V_4. \tag{E1}$$

Here the four vertex operators are located at

$$\begin{aligned}(0,0):\ V_1 &= e^{-\frac{\alpha_1-\alpha_2}{2\pi}\phi(0,0)},\\ (L_A,0):\ V_2 &= e^{\frac{\alpha_1-\alpha_2}{2\pi}\phi(L_A,0)},\\ (0,\beta):\ V_3 &= e^{\frac{\alpha_1-\alpha_2}{2\pi}\phi(0,\beta)},\\ (L_A,\beta):\ V_4 &= e^{-\frac{\alpha_1-\alpha_2}{2\pi}\phi(L_A,\beta)}.\end{aligned}$$

Notice that while $\mathrm{Tr}\rho^2 = \frac{\mathrm{Tr}e^{-2\beta H}}{Z^2}$, we have

$$\mathrm{Tr}\rho_m^2 = \frac{\mathrm{Tr}e^{-2\beta H}\int\frac{d\alpha_1 d\alpha_2}{(2\pi)^2}V_1V_2V_3V_4}{Z^2}. \tag{E2}$$

The object of interest is entropy change, which can be written as $\Delta S_2 = -\ln\frac{\mathrm{Tr}\rho_m^2}{\mathrm{Tr}\rho^2}$ resulting in Eq. (E1). We conclude that ΔS_2 is determined entirely by the four-point function:

$$\Delta S_2 = -\ln\int\frac{d\alpha_1 d\alpha_2}{(2\pi)^2}V_1V_2V_3V_4. \tag{E3}$$

The four-point function can be calculated by mapping the cylinder to the complex plane, on which there is a closed formula for the multipoint correlation function. As shown in the following subsection,

$$V_1V_2V_3V_4 = \left(\frac{2\beta\tanh\frac{\pi L_A}{2\beta}}{\pi}\right)^{-\frac{(\alpha_1-\alpha_2)^2}{\pi^2}}. \tag{E4}$$

The integration over α_1 and α_2 can be done exactly. In the following, we consider two temperature regions separately, $T = 0$ and $\frac{1}{L_A} \ll T \ll \Lambda$. (a) $T = 0$. In this limit

$$\lim_{\beta\to\infty}\left(\frac{2\beta\tanh\frac{\pi L_A}{2\beta}}{\pi}\right) = L_A. \tag{E5}$$

The integration over α_1 and α_2 gives the aforementioned double log scaling:

$$\Delta S_2 = \tfrac{1}{2}\ln\ln L_A + \mathrm{const}. \tag{E6}$$

(b) $\frac{1}{L_A} \ll T \ll \Lambda \sim t$. In this regime $\tanh\frac{\pi L_A}{2\beta} \cong 1$ and the four-point function depends on β solely. The same integration gives

$$\Delta S_2 \sim \tfrac{1}{2}\ln\ln\frac{\mathrm{const}}{T} + \mathrm{const}'. \tag{E7}$$

The CFT results hold true only when $T \ll \Lambda$. In Fig. 4 of the main text we plot the result of exact integration of Eq. (E4) over the α_i's.

Derivation of Eq. (E4)

Here we provide the details of the calculation of the four-point correlation function of vertex operators on the cylinder, Eq. (E4).

We introduce complex coordinate $w = x + i\tau$, and map the cylinder to the complex plane by

$$z = e^{\frac{\pi}{\beta}w}. \tag{E8}$$

The operators are now inserted at $(1,0), (-1,0), (x,0), (-x,0)$, where (x,y) denotes a point on a complex plane with $z = x + iy$. Here $x = e^{\frac{\pi}{\beta}L_A}$. The multipoint correlation function of vertex operators $V^A = e^{iA\phi}$,

where $A = \pm\frac{\alpha_i}{2\pi}$ is given by

$$V^{A_1}(z_1,\bar{z}_1)\cdots V^{A_n}(z_n,\bar{z}_n) = \prod_{i<j}|z_i - z_j|^{2A_iA_j}. \tag{E9}$$

According to the above formula, we get

$$V_1(z_1,\bar{z}_1)V_2(z_2,\bar{z}_2)V_3(z_3,\bar{z}_3)V_4(z_4,\bar{z}_4) = (x-1)^{-\frac{(\alpha_1-\alpha_2)^2}{\pi^2}}(x+1)^{\frac{(\alpha_1-\alpha_2)^2}{\pi^2}}(2x)^{-\frac{(\alpha_1-\alpha_2)^2}{2\pi^2}}2^{-\frac{(\alpha_1-\alpha_2)^2}{2\pi^2}}. \tag{E10}$$

To get the correlation function on the cylinder, we have to add the factor associated with the conformal transformation:

$$\phi'(w,\bar{w}) = \left|\frac{\partial z}{\partial w}\right|^{2h}\phi(z,\bar{z}), \tag{E11}$$

where $z = e^{\frac{\pi}{\beta}w}$ and $\frac{\partial z}{\partial w} = \frac{\pi}{\beta}z$. We conclude that the four-point function on the cylinder is given by

$$\begin{aligned} &V_1(w_1,\bar{w}_1)V_2(w_2,\bar{w}_2)V_3(w_3,\bar{w}_3)V_4(w_4,\bar{w}_4) \\ &= (x-1)^{-\frac{(\alpha_1-\alpha_2)^2}{\pi^2}}(x+1)^{\frac{(\alpha_1-\alpha_2)^2}{\pi^2}}(2x)^{-\frac{(\alpha_1-\alpha_2)^2}{2\pi^2}} \\ &2^{-\frac{(\alpha_1-\alpha_2)^2}{2\pi^2}}\left(\frac{\pi}{\beta}x\right)^{\frac{(\alpha_1-\alpha_2)^2}{2\pi^2}}\left(\frac{\pi}{\beta}\right)^{\frac{(\alpha_1-\alpha_2)^2}{2\pi^2}} \\ &= \left(\frac{2\beta}{\pi}\frac{x-1}{x+1}\right)^{-\frac{(\alpha_1-\alpha_2)^2}{\pi^2}} \\ &= \left(\frac{2\beta}{\pi}\tanh\frac{\pi L_A}{2\beta}\right)^{-\frac{(\alpha_1-\alpha_2)^2}{\pi^2}}. \end{aligned} \tag{E12}$$

[1] P. Calabrese and J. Cardy, Entanglement entropy and quantum field theory, J. Stat. Mech.: Theory Exp. (2004) P06002.

[2] L. Amico, R. Fazio, A. Osterloh, and V. Vedral, Entanglement in many-body systems, Rev. Mod. Phys. **80**, 517 (2008).

[3] R. Horodecki, P. Horodecki, M. Horodecki, and K. Horodecki, Quantum entanglement, Rev. Mod. Phys. **81**, 865 (2009).

[4] J. Eisert, M. Cramer, and M. B. Plenio, Colloquium: Area laws for the entanglement entropy, Rev. Mod. Phys. **82**, 277 (2010).

[5] N. Laflorencie, Quantum entanglement in condensed matter systems, Phys. Rep. **646**, 1 (2016).

[6] L. Gurvits, Classical deterministic complexity of Edmonds' problem and quantum entanglement, in Proceedings of the Thirty-Fifth Annual ACM Symposium on Theory of Computing, 2003 (unpublished), pp. 10–19.

[7] S. Gharibian, Strong np-hardness of the quantum separability problem, arXiv:0810.4507.

[8] L. Qian, L. Chen, and D. Chu, Separability of symmetric states and Vandermonde decomposition, New J. Phys. **22**, 033019 (2020).

[9] A. Peres, Separability Criterion for Density Matrices, Phys. Rev. Lett. **77**, 1413 (1996).

[10] G. Vidal and R. F. Werner, Computable measure of entanglement, Phys. Rev. A **65**, 032314 (2002).

[11] M. B. Plenio, Logarithmic Negativity: A Full Entanglement Monotone that is Not Convex, Phys. Rev. Lett. **95**, 090503 (2005).

[12] T.-C. Lu and T. Grover, Structure of quantum entanglement at a finite temperature critical point, Phys. Rev. Research **2**, 043345 (2020).

[13] K. Macieszczak, E. Levi, T. Macrì, I. Lesanovsky, and J. P. Garrahan, Coherence, entanglement, and quantumness in closed and open systems with conserved charge, with an application to many-body localization, Phys. Rev. A **99**, 052354 (2019).

[14] M. B. Plenio and S. S. Virmani, An introduction to entanglement theory, in *Quantum Information and Coherence* (Springer, New York, 2014), pp. 173–209.

[15] M. A. Nielsen and I. L. Chuang, *Quantum Computation and Quantum Information* (Cambridge University Press, Cambridge, 2002).

[16] M. Goldstein and E. Sela, Symmetry-Resolved Entanglement in Many-Body Systems, Phys. Rev. Lett. **120**, 200602 (2018).

[17] J. C. Xavier, F. C. Alcaraz, and G Sierra, Equipartition of the entanglement entropy, Phys. Rev. B **98**, 041106(R) (2018).

[18] A. Lukin, M. Rispoli, R. Schittko, M Eric Tai, A. M. Kaufman, S. Choi, V. Khemani, J. Léonard, and M. Greiner, Probing entanglement in a many-body-localized system, Science **364**, 256 (2019).

[19] R. Bonsignori, P. Ruggiero, and P. Calabrese, Symmetry resolved entanglement in free fermionic systems, J. Phys. A **52**, 475302 (2019).

[20] T. Rakovszky, C. W. von Keyserlingk, and F. Pollmann, Entanglement growth after inhomogeneous quenches, Phys. Rev. B **100**, 125139 (2019).

[21] M. Kiefer-Emmanouilidis, R. Unanyan, M. Fleischhauer, and J. Sirker, Evidence for Unbounded Growth of the Number Entropy in Many-Body Localized Phases, Phys. Rev. Lett. **124**, 243601 (2020).

[22] P. Calabrese, J. Dubail, and S. Murciano, Symmetry-resolved entanglement entropy in Wess-Zumino-Witten models, J. High Energy Phys. 10 (2021) 067.

[23] H. M. Wiseman and J. A. Vaccaro, Entanglement of Indistinguishable Particles Shared Between two Parties, Phys. Rev. Lett. **91**, 097902 (2003).

[24] H. Barghathi, C. M. Herdman, and A. Del Maestro, Rényi Generalization of the Accessible Entanglement Entropy, Phys. Rev. Lett. **121**, 150501 (2018).

[25] H. Barghathi, E. Casiano-Diaz, and A. Del Maestro, Operationally accessible entanglement of one-dimensional spinless fermions, Phys. Rev. A **100**, 022324 (2019).

[26] E. Cornfeld, M. Goldstein, and E. Sela, Imbalance entanglement: Symmetry decomposition of negativity, Phys. Rev. A **98**, 032302 (2018).

[27] N. Feldman and M. Goldstein, Dynamics of charge-resolved entanglement after a local quench, Phys. Rev. B **100**, 235146 (2019).

[28] D. X. Horváth and P. Calabrese, Symmetry resolved entanglement in integrable field theories via form factor bootstrap, J. High Energy Phys. 11 (2020) 131.

[29] S. Fraenkel and M. Goldstein, Symmetry resolved entanglement: exact results in 1D and beyond, J. Stat. Mech.: Theory Exp. (2020) 033106.
[30] A. Neven, J. Carrasco, V. Vitale, C. Kokail, A. Elben, M. Dalmonte, P. Calabrese, P. Zoller, B. Vermersch, R. Kueng, and B. Kraus, Symmetry-resolved entanglement detection using partial transpose moments, npj Quantum Inf. **7**, 152 (2021).
[31] S. Fraenkel and M. Goldstein, Entanglement measures in a nonequilibrium steady state: Exact results in one dimension, SciPost Phys. **11**, 085 (2021).
[32] S. Murciano, R. Bonsignori, and P. Calabrese, Symmetry decomposition of negativity of massless free fermions, SciPost Phys. **10**, 111 (2021).
[33] V. Vitale, A. Elben, R. Kueng, A. Neven, J. Carrasco, B. Kraus, P. Zoller, P. Calabrese, B. Vermersch, and M. Dalmonte, Symmetry-resolved dynamical purification in synthetic quantum matter, SciPost Phys. **12**, 106 (2022).
[34] D. Azses, R. Haenel, Y. Naveh, R. Raussendorf, E. Sela, and E. G. Dalla Torre, Identification of Symmetry-Protected Topological States on Noisy Quantum Computers, Phys. Rev. Lett. **125**, 120502 (2020).
[35] D. Azses and E. Sela, Symmetry-resolved entanglement in symmetry-protected topological phases, Phys. Rev. B **102**, 235157 (2020).
[36] D. Azses, E. G. Dalla Torre, and E. Sela, Observing floquet topological order by symmetry resolution, Phys. Rev. B **104**, L220301 (2021).
[37] N. E. Sherman, T. Devakul, M. B. Hastings, and R. R. P. Singh, Nonzero-temperature entanglement negativity of quantum spin models: Area law, linked cluster expansions, and sudden death, Phys. Rev. E **93**, 022128 (2016).
[38] H. Shapourian, K. Shiozaki, and S. Ryu, Partial time-reversal transformation and entanglement negativity in fermionic systems, Phys. Rev. B **95**, 165101 (2017).
[39] H. Shapourian and S. Ryu, Entanglement negativity of fermions: Monotonicity, separability criterion, and classification of few-mode states, Phys. Rev. A **99**, 022310 (2019).
[40] H. Shapourian, P. Ruggiero, S. Ryu, and P. Calabrese, Twisted and untwisted negativity spectrum of free fermions, SciPost Phys **7**, 037 (2019).
[41] M. Fagotti and P. Calabrese, Entanglement entropy of two disjoint blocks in XY chains, J. Stat. Mech.: Theory Exp. (2010) P04016.
[42] R. Islam, R. Ma, P. M. Preiss, M Eric Tai, A. Lukin, M. Rispoli, and M. Greiner, Measuring entanglement entropy in a quantum many-body system, Nature (London) **528**, 77 (2015).
[43] J. Gray, L. Banchi, A. Bayat, and S. Bose, Measuring Entanglement Negativity, Phys. Rev. Lett. **121**, 150503 (2018).
[44] A. Elben, B. Vermersch, C. F. Roos, and P. Zoller, Statistical correlations between locally randomized measurements: A toolbox for probing entanglement in many-body quantum states, Phys. Rev. A **99**, 052323 (2019).
[45] N. Hartman, C. Olsen, S. Lüscher, M. Samani, S. Fallahi, G. C. Gardner, M. Manfra, and J. Folk, Direct entropy measurement in a mesoscopic quantum system, Nat. Phys. **14**, 1083 (2018).
[46] Y. Kleeorin, H. Thierschmann, H. Buhmann, A. Georges, L. W. Molenkamp, and Y. Meir, How to measure the entropy of a mesoscopic system via thermoelectric transport, Nat. Commun. **10**, 5801 (2019).
[47] E. Sela, Y. Oreg, S. Plugge, N. Hartman, S. Lüscher, and J. Folk, Detecting the Universal Fractional Entropy of Majorana Zero Modes, Phys. Rev. Lett. **123**, 147702 (2019).
[48] C. Han, A. K. Mitchell, Z. Iftikhar, Y. Kleeorin, A. Anthore, F. Pierre, Y. Meir, and E. Sela, Extracting entropy of exotic quasiparticles from conductance measurements, arXiv:2108.12878.
[49] I. L. Aleiner, N. S. Wingreen, and Y. Meir, Dephasing and the Orthogonality Catastrophe in Tunneling Through a Quantum Dot: The Which Path? Interferometer, Phys. Rev. Lett. **79**, 3740 (1997).
[50] Y. Levinson, Dephasing in a quantum dot due to coupling with a quantum point contact, Europhys. Lett. **39**, 299 (1997).
[51] H. F. Song, S. Rachel, and K. Le Hur, General relation between entanglement and fluctuations in one dimension, Phys. Rev. B **82**, 012405 (2010).
[52] H. F. Song, C. Flindt, S. Rachel, I. Klich, and K. Le Hur, Entanglement entropy from charge statistics: Exact relations for noninteracting many-body systems, Phys. Rev. B **83**, 161408(R) (2011).
[53] S. Rachel, N. Laflorencie, H. F. Song, and K. Le Hur, Detecting Quantum Critical Points using Bipartite Fluctuations, Phys. Rev. Lett. **108**, 116401 (2012).
[54] A. Nir, E. Sela, R. Beck, and Y. Bar-Sinai, Machine-learning iterative calculation of entropy for physical systems, Proc. Natl. Acad. Sci. USA **117**, 30234 (2020).